



HAL
open science

Equilibrated stress reconstructions for linear elasticity problems with application to a posteriori error analysis

Rita Riedlbeck, Daniele Di Pietro, Alexandre Ern

► To cite this version:

Rita Riedlbeck, Daniele Di Pietro, Alexandre Ern. Equilibrated stress reconstructions for linear elasticity problems with application to a posteriori error analysis. Clément Cancès; Pascal Omnes. Finite Volumes for Complex Applications VIII – Methods and Theoretical Aspects, 199, pp.293-301, 2017, Springer Proceedings in Mathematics & Statistics, 978-3-319-57397-7. 10.1007/978-3-319-57397-7. hal-01433841v2

HAL Id: hal-01433841

<https://hal.science/hal-01433841v2>

Submitted on 16 Feb 2017

HAL is a multi-disciplinary open access archive for the deposit and dissemination of scientific research documents, whether they are published or not. The documents may come from teaching and research institutions in France or abroad, or from public or private research centers.

L'archive ouverte pluridisciplinaire **HAL**, est destinée au dépôt et à la diffusion de documents scientifiques de niveau recherche, publiés ou non, émanant des établissements d'enseignement et de recherche français ou étrangers, des laboratoires publics ou privés.

Equilibrated stress reconstructions for linear elasticity problems with application to a posteriori error analysis

Rita Riedlbeck, Daniele A. Di Pietro, and Alexandre Ern

Abstract We present an a posteriori error estimate for the linear elasticity problem. The estimate is based on an equilibrated reconstruction of the Cauchy stress tensor, which is obtained from mixed finite element solutions of local Neumann problems. We propose two different reconstructions: one using Arnold–Winther mixed finite element spaces providing a symmetric stress tensor, and one using Arnold–Falk–Winther mixed finite element spaces with a weak symmetry constraint. The performance of the estimate is illustrated on a numerical test with analytical solution.

Key words: a posteriori error estimate, linear elasticity, equilibrated stress reconstruction, Arnold–Winther finite element, Arnold–Falk–Winther finite element

MSC (2010): 65N15, 74S05

1 Introduction

We consider the linear elasticity problem on a simply connected polygon $\Omega \subset \mathbb{R}^2$:

$$-\nabla \cdot \boldsymbol{\sigma}(\mathbf{u}) = \mathbf{f} \quad \text{in } \Omega, \quad (1a)$$

$$\mathbf{u} = \mathbf{0} \quad \text{on } \partial\Omega, \quad (1b)$$

Rita Riedlbeck

IMAG, University of Montpellier, Place Eugène Bataillon, 34090 Montpellier, France

EDF R&D, IMSIA, 7, Boulevard Gaspard Monge, 91120 Palaiseau, France

e-mail: rita.riedlbeck@edf.fr

Daniele A. Di Pietro

IMAG, University of Montpellier, Place Eugène Bataillon, 34090 Montpellier, France

e-mail: daniele.di-pietro@umontpellier.fr

The work of D. A. Di Pietro was supported by ANR grant HHOMM (ANR-15-CE40-0005)

Alexandre Ern

Université Paris-Est, CERMICS (ENPC), 6–8, Avenue B. Pascal, 77455 Marne la Vallée, France

e-mail: alexandre.ern@enpc.fr

where $\mathbf{u} : \Omega \rightarrow \mathbb{R}^2$ the displacement, and $\mathbf{f} : \Omega \rightarrow \mathbb{R}^2$ the volumetric body force. The Cauchy stress tensor $\boldsymbol{\sigma}$ is given by Hooke's law $\boldsymbol{\sigma}(\mathbf{u}) = \lambda \operatorname{tr}(\boldsymbol{\varepsilon}(\mathbf{u}))\mathbf{I} + 2\mu\boldsymbol{\varepsilon}(\mathbf{u})$, where λ and μ are the Lamé parameters, and the symmetric gradient $\boldsymbol{\varepsilon}(\mathbf{u}) = \frac{1}{2}((\nabla\mathbf{u})^T + \nabla\mathbf{u})$ describes the infinitesimal strain.

In many applications, this problem is approximated using H^1 -conforming finite elements. It is well known that, in contrast to the analytical solution, the resulting discrete stress tensor does not have continuous normal components across mesh interfaces, and its divergence is not locally in equilibrium with the source term \mathbf{f} on mesh cells. In this paper we propose an a posteriori error estimate based on stress tensor functions which are reconstructed from the discrete stress tensor such that they verify both of the above properties. Such equilibrated-flux a posteriori error estimates offer several advantages. First, error upper bounds are obtained with fully computable constants. Second, polynomial-degree robustness can be achieved for the Poisson problem in [4, 11], for linear elasticity in [9], and for the related Stokes problem in [7]. Third, they allow one to distinguish among various error components, e.g., discretization, linearization, and algebraic solver error components, and to equilibrate adaptively these components in the iterative solution of nonlinear problems [10]. An advantage for more general problems in solid mechanics is that the stress reconstruction is based on the discrete stress (not the displacement) and thus the estimate does not depend on the mechanical behaviour law.

We present two stress reconstructions. Both use mixed finite elements on cell patches around mesh vertices, as proposed for the Poisson problem in [8, 5]. The first one was introduced in [15] and uses the Arnold–Winther (AW) mixed finite element spaces [3] providing a symmetric stress tensor. The second one follows the same approach, but imposing the symmetry only weakly and using the Arnold–Falk–Winther (AFW) mixed finite element spaces [2]. Element-wise reconstructions of equilibrated stress tensors from local Neumann problems can be found in [13, 1, 12], whereas direct prescription of the degrees of freedom in the AW finite element space is considered in [14].

2 Setting

We denote by $L^2(\Omega)$ the space of square-integrable functions taking values in \mathbb{R} , and by (\cdot, \cdot) and $\|\cdot\|$ the corresponding inner product and norm. $H^1(\Omega)$ stands for the Sobolev space composed of $L^2(\Omega)$ functions with weak gradients in $[L^2(\Omega)]^2$ and $H_0^1(\Omega)$ for its zero-trace subspace. The weak formulation of problem (1) reads: find $\mathbf{u} \in [H_0^1(\Omega)]^2$ such that

$$(\boldsymbol{\sigma}(\mathbf{u}), \boldsymbol{\varepsilon}(\mathbf{v})) = (\mathbf{f}, \mathbf{v}) \quad \forall \mathbf{v} \in [H_0^1(\Omega)]^2. \quad (2)$$

The discretization of (2) is based on a conforming triangulation \mathcal{T}_h of Ω , verifying the minimum angle condition. We will use a conforming finite element method of order $p \geq 2$. Let $\mathbb{P}^p(\mathcal{T}_h) := \{v \in L^2(\Omega) \mid \forall T \in \mathcal{T}_h \ v|_T \in \mathbb{P}^p(T)\}$, where $\mathbb{P}^p(T)$

is the space of polynomials on T of degree less than or equal to p . For the sake of simplicity we assume that \mathbf{f} lies in $[\mathbb{P}^{p-1}(\mathcal{T}_h)]^2$. Then the discrete problem reads: find $\mathbf{u}_h \in [H_0^1(\Omega)]^2 \cap [\mathbb{P}^p(\mathcal{T}_h)]^2$ such that

$$(\boldsymbol{\sigma}(\mathbf{u}_h), \boldsymbol{\varepsilon}(\mathbf{v}_h)) = (\mathbf{f}, \mathbf{v}_h) \quad \forall \mathbf{v}_h \in [H_0^1(\Omega)]^2 \cap [\mathbb{P}^p(\mathcal{T}_h)]^2. \quad (3)$$

3 A Posteriori Error Estimate

In this section, we derive an upper bound on the error between the analytical solution of (2) and an arbitrary function $\mathbf{u}_h \in [H_0^1(\Omega)]^2 \cap [\mathbb{P}^p(\mathcal{T}_h)]^2$. We will measure this error in the energy norm

$$\|\mathbf{v}\|_{\text{en}}^2 := (\boldsymbol{\sigma}(\mathbf{v}), \boldsymbol{\varepsilon}(\mathbf{v})) = 2\mu\|\boldsymbol{\varepsilon}(\mathbf{v})\|^2 + \lambda\|\nabla \cdot \mathbf{v}\|^2 \geq 2\mu C_K \|\nabla \mathbf{v}\|^2, \quad (4)$$

where the last bound follows from $\lambda \geq 0$ and Korn's inequality. Owing to (1b), we have $C_K = \frac{1}{2}$ (this value would have been different if we had chosen mixed boundary conditions). We start by introducing reconstructed stress tensors that are more "physical" than $\boldsymbol{\sigma}(\mathbf{u}_h)$, which in general does not lie in $\mathbf{H}(\text{div}, \Omega) = \{\boldsymbol{\tau} \in [L^2(\Omega)]^{2 \times 2} \mid \nabla \cdot \boldsymbol{\tau} \in [L^2(\Omega)]^2\}$ and thus cannot verify the equilibrium equation (1a). Unlike $\boldsymbol{\sigma}(\mathbf{u}_h)$, however, these reconstructed tensors may not be symmetric.

Definition 1 (Equilibrated stress reconstruction). We call *equilibrated stress reconstruction* any function $\boldsymbol{\sigma}_h \in \mathbf{H}(\text{div}, \Omega)$ constructed from $\boldsymbol{\sigma}(\mathbf{u}_h)$ such that

$$(-\nabla \cdot \boldsymbol{\sigma}_h, \mathbf{z})_T = (\mathbf{f}, \mathbf{z})_T \quad \forall \mathbf{z} \in \mathbf{RM} \forall T \in \mathcal{T}_h, \quad (5)$$

where $\mathbf{RM} := \{\mathbf{b} + c(x_2, -x_1)^T \mid \mathbf{b} \in \mathbb{R}^2, c \in \mathbb{R}\}$ is the space of rigid body motions.

Theorem 1 (A posteriori error estimate). Let $\mathbf{u} \in [H_0^1(\Omega)]^2$ solve (2) and $\mathbf{u}_h \in [H_0^1(\Omega)]^2$ be arbitrary. Let $\boldsymbol{\sigma}_h$ be a stress reconstruction verifying Definition 1. Then

$$\|\mathbf{u} - \mathbf{u}_h\|_{\text{en}} \leq \mu^{-1/2} \left(\sum_{T \in \mathcal{T}_h} \left(\frac{h_T}{\pi} \|\mathbf{f} + \nabla \cdot \boldsymbol{\sigma}_h\|_T + \|\boldsymbol{\sigma}_h - \boldsymbol{\sigma}(\mathbf{u}_h)\|_T \right)^2 \right)^{1/2}. \quad (6)$$

Proof. From (4) and the symmetry of $\boldsymbol{\sigma}(\mathbf{u} - \mathbf{u}_h)$, we infer that

$$\begin{aligned} \|\mathbf{u} - \mathbf{u}_h\|_{\text{en}} &= \left(\boldsymbol{\sigma}(\mathbf{u} - \mathbf{u}_h), \frac{\boldsymbol{\varepsilon}(\mathbf{u} - \mathbf{u}_h)}{\|\mathbf{u} - \mathbf{u}_h\|_{\text{en}}} \right) \leq \mu^{-1/2} \left(\boldsymbol{\sigma}(\mathbf{u} - \mathbf{u}_h), \frac{\boldsymbol{\varepsilon}(\mathbf{u} - \mathbf{u}_h)}{\|\nabla(\mathbf{u} - \mathbf{u}_h)\|} \right) \\ &\leq \mu^{-1/2} \sup_{\mathbf{v} \in [H_0^1(\Omega)]^2; \|\nabla \mathbf{v}\|=1} (\boldsymbol{\sigma}(\mathbf{u} - \mathbf{u}_h), \nabla \mathbf{v}). \end{aligned} \quad (7)$$

Fix $\mathbf{v} \in [H_0^1(\Omega)]^2$, such that $\|\nabla \mathbf{v}\| = 1$. Using the fact that \mathbf{u} verifies (2), and inserting $(\nabla \cdot \boldsymbol{\sigma}_h, \mathbf{v}) + (\boldsymbol{\sigma}_h, \nabla \mathbf{v}) = 0$ into the term inside the supremum yields

$$(\boldsymbol{\sigma}(\mathbf{u} - \mathbf{u}_h), \nabla \mathbf{v}) = (\mathbf{f}, \mathbf{v}) - (\boldsymbol{\sigma}(\mathbf{u}_h), \nabla \mathbf{v}) = (\mathbf{f} + \nabla \cdot \boldsymbol{\sigma}_h, \mathbf{v}) + (\boldsymbol{\sigma}_h - \boldsymbol{\sigma}(\mathbf{u}_h), \nabla \mathbf{v}). \quad (8)$$

For the first term in the right hand side of (8) we use (5) to insert the mean value $\Pi_T^0 \mathbf{v}$ of \mathbf{v} on T , the Cauchy–Schwarz inequality, and the Poincaré inequality $\|\mathbf{v} - \Pi_T^0 \mathbf{v}\|_T \leq \frac{h_T}{\pi} \|\nabla \mathbf{v}\|_T$ on simplexes $T \in \mathcal{T}_h$, and obtain

$$|(\mathbf{f} + \nabla \cdot \boldsymbol{\sigma}_h, \mathbf{v})| \leq \left| \sum_{T \in \mathcal{T}_h} (\mathbf{f} + \nabla \cdot \boldsymbol{\sigma}_h, \mathbf{v} - \Pi_T^0 \mathbf{v})_T \right| \leq \sum_{T \in \mathcal{T}_h} \frac{h_T}{\pi} \|\mathbf{f} + \nabla \cdot \boldsymbol{\sigma}_h\|_T \|\nabla \mathbf{v}\|_T,$$

whereas the Cauchy–Schwarz inequality applied to the second term directly yields

$$|(\boldsymbol{\sigma}_h - \boldsymbol{\sigma}(\mathbf{u}_h), \nabla \mathbf{v})| \leq \sum_{T \in \mathcal{T}_h} \|\boldsymbol{\sigma}_h - \boldsymbol{\sigma}(\mathbf{u}_h)\|_T \|\nabla \mathbf{v}\|_T.$$

Inserting these results in (7) and again applying the Cauchy–Schwarz inequality yields the result. \square

4 Stress Tensor Reconstructions

The set of vertices of the mesh \mathcal{T}_h is denoted by \mathcal{V}_h ; it is decomposed into interior vertices $\mathcal{V}_h^{\text{int}}$ and boundary vertices $\mathcal{V}_h^{\text{ext}}$. For all $a \in \mathcal{V}_h$, \mathcal{T}_a is the patch of elements sharing the vertex a , ω_a the corresponding open subdomain in Ω , \mathbf{n}_{ω_a} its unit outward normal vector, and ψ_a the piecewise affine “hat” function which takes the value 1 at the vertex a and zero at all the other vertices. For all $T \in \mathcal{T}_h$, \mathcal{V}_T denotes the set of vertices of T and h_T its diameter.

From now on, \mathbf{u}_h denotes the solution of (3). The goal is to minimize the error estimate (6) avoiding global computations. As a result, both of the proposed reconstructions are based on local minimization problems on the patches ω_a :

$$\boldsymbol{\sigma}_h^a := \arg \min_{\boldsymbol{\tau}_h \in \Sigma_h^a, \nabla \cdot \boldsymbol{\tau}_h = \boldsymbol{\psi}_a \mathbf{f}} \|\boldsymbol{\tau}_h - \boldsymbol{\psi}_a \boldsymbol{\sigma}(\mathbf{u}_h)\|_{\omega_a}, \quad (9)$$

where we define Σ_h^a separately for each construction and add a weak symmetry constraint in the second (AFW) construction. The global reconstructed stress tensor $\boldsymbol{\sigma}_h$ is then obtained assembling the local solutions $\boldsymbol{\sigma}_h^a$.

4.1 Arnold–Winther Stress Reconstruction

For each element $T \in \mathcal{T}_h$, the local AW spaces of degree $k \geq 1$ are defined by [3]

$$\mathbf{S}_T^{\text{AW}} := \{\boldsymbol{\tau} \in [\mathbb{P}^{k+2}(T)]_{\text{sym}}^{2 \times 2} \mid \nabla \cdot \boldsymbol{\tau} \in [\mathbb{P}^k(T)]^2\}, \quad \mathbf{V}_T^{\text{AW}} := [\mathbb{P}^k(T)]^2,$$

where $[\mathbb{P}^k(T)]_{\text{sym}}^{2 \times 2}$ denotes the subspace of $[\mathbb{P}^k(T)]^{2 \times 2}$ composed of symmetric-valued tensors. Figure 1 shows the corresponding 24 degrees of freedom for the

symmetric stress tensor in the lowest-order case $k = 1$: the values of the three components at each vertex of the triangle, the values of the moments of degree zero and 1 of the normal components each edge, and the value of the moment of degree zero of each component on the triangle. On a patch ω_a , the AW mixed finite element spaces are defined as

$$\begin{aligned}\mathbf{S}_h^{\text{AW}}(\omega_a) &:= \{\boldsymbol{\tau}_h \in \mathbf{H}(\text{div}, \omega_a) \cap [\mathbb{P}^{k+2}(T)]_{\text{sym}}^{2 \times 2} \mid \boldsymbol{\tau}_h|_T \in \mathbf{S}_T^{\text{AW}} \forall T \in \mathcal{T}_a\}, \\ \mathbf{V}_h^{\text{AW}}(\omega_a) &:= \{\mathbf{v}_h \in [L^2(\omega_a)]^2 \mid \mathbf{v}_h|_T \in \mathbf{V}_T^{\text{AW}} \forall T \in \mathcal{T}_a\}.\end{aligned}$$

Let now $k := p - 1$. We need to consider subspaces where a zero normal component is enforced on the stress tensor. Since the boundary condition in the exact problem prescribes the displacement and not the normal stress, we distinguish the case whether a is an interior vertex or a boundary vertex. For $a \in \mathcal{V}_h^{\text{int}}$, we set

$$\Sigma_h^a := \{\boldsymbol{\tau}_h \in \mathbf{S}_h^{\text{AW}}(\omega_a) \mid \boldsymbol{\tau}_h \mathbf{n}_{\omega_a} = \mathbf{0} \text{ on } \partial\omega_a, \boldsymbol{\tau}_h(b) = \mathbf{0} \forall b \in \mathcal{V}_{\omega_a}^{\text{ext}}\}, \quad (12a)$$

$$\mathbf{V}_h^a := \{\mathbf{v}_h \in \mathbf{V}_h^{\text{AW}}(\omega_a) \mid (\mathbf{v}_h, \mathbf{z})_{\omega_a} = 0 \forall \mathbf{z} \in \mathbf{RM}\}, \quad (12b)$$

with $\mathcal{V}_{\omega_a}^{\text{ext}} = \mathcal{V}_h \cap \partial\omega_a$, and for $a \in \mathcal{V}_h^{\text{ext}}$, we set

$$\Sigma_h^a := \{\boldsymbol{\tau}_h \in \mathbf{S}_h^{\text{AW}}(\omega_a) \mid \boldsymbol{\tau}_h \mathbf{n}_{\omega_a} = \mathbf{0} \text{ on } \partial\omega_a \setminus \partial\Omega, \boldsymbol{\tau}_h(b) = \mathbf{0} \forall b \in \mathcal{V}_{\omega_a}^{\text{ext}}\}, \quad (13a)$$

$$\mathbf{V}_h^a := \mathbf{V}_h^{\text{AW}}(\omega_a), \quad (13b)$$

with $\mathcal{V}_{\omega_a}^{\text{ext}} = \mathcal{V}_h \cap (\partial\omega_a \setminus \partial\Omega)$. As argued in [3], the nodal degrees of freedom on $\partial\omega_a$ are set to zero if the vertex separates two edges where the normal stress is zero.

Construction 1 (AW stress reconstruction) Find $\boldsymbol{\sigma}_h^a \in \Sigma_h^a$ and $\mathbf{r}_h^a \in \mathbf{V}_h^a$ such that for all $(\boldsymbol{\tau}_h, \mathbf{v}_h) \in \Sigma_h^a \times \mathbf{V}_h^a$,

$$(\boldsymbol{\sigma}_h^a, \boldsymbol{\tau}_h)_{\omega_a} + (\mathbf{r}_h^a, \nabla \cdot \boldsymbol{\tau}_h)_{\omega_a} = (\boldsymbol{\psi}_a \boldsymbol{\sigma}(\mathbf{u}_h), \boldsymbol{\tau}_h)_{\omega_a}, \quad (14a)$$

$$(\nabla \cdot \boldsymbol{\sigma}_h^a, \mathbf{v}_h)_{\omega_a} = (-\boldsymbol{\psi}_a \mathbf{f} + \boldsymbol{\sigma}(\mathbf{u}_h) \nabla \boldsymbol{\psi}_a, \mathbf{v}_h)_{\omega_a}. \quad (14b)$$

Then, extending $\boldsymbol{\sigma}_h^a$ by zero outside ω_a , set $\boldsymbol{\sigma}_h := \sum_{a \in \mathcal{V}_h} \boldsymbol{\sigma}_h^a$.

Using the definitions (12) and (13), the formulation (14) is equivalent to (9). For interior vertices, the source term in (14a) has to verify the Neumann compatibility condition

$$(-\boldsymbol{\psi}_a \mathbf{f} + \boldsymbol{\sigma}(\mathbf{u}_h) \nabla \boldsymbol{\psi}_a, \mathbf{z})_{\omega_a} = 0 \quad \forall \mathbf{z} \in \mathbf{RM}. \quad (15)$$

Taking $\boldsymbol{\psi}_a \mathbf{z}$ as a test function in (3), we see that (15) holds.

4.2 Arnold–Falk–Winther Stress Reconstruction

For each element $T \in \mathcal{T}_h$, the local AFW mixed finite element spaces [2] of degree $k \geq 1$ hinge on the Brezzi–Douglas–Marini mixed finite element spaces [6] for each line of the stress tensor and are defined by

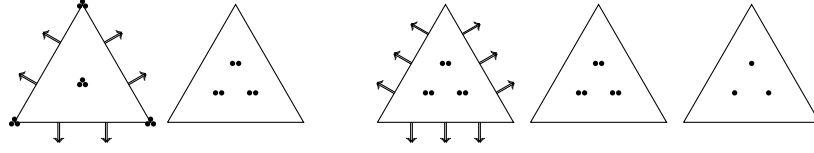


Fig. 1 Element diagrams for $(\mathbf{S}_T^{\text{AW}}, \mathbf{V}_T^{\text{AW}})$ with $k = 1$ (left) and $(\mathbf{S}_T^{\text{AFW}}, \mathbf{V}_T^{\text{AFW}}, \Lambda_T)$ with $k = 2$ (right)

$$\mathbf{S}_T^{\text{AFW}} := [\mathbb{P}^k(T)]^{2 \times 2}, \quad \mathbf{V}_T^{\text{AFW}} := [\mathbb{P}^{k-1}(T)]^2, \quad \Lambda_T := \{\boldsymbol{\mu} \in [\mathbb{P}^{k-1}(T)]^{2 \times 2} \mid \boldsymbol{\mu} = -\boldsymbol{\mu}^T\}.$$

On a patch ω_a the global space $\mathbf{S}_h^{\text{AFW}}(\omega_a)$ is the subspace of $\mathbf{H}(\text{div}, \omega_a)$ composed of functions belonging piecewise to $\mathbf{S}_T^{\text{AFW}}$. The spaces $\mathbf{V}_h^{\text{AFW}}(\omega_a)$ and $\Lambda_h(\omega_a)$ consist of functions lying piecewise in \mathbf{V}_T and Λ_T respectively, with no continuity conditions between two elements.

As for the previous construction, we define subspaces with zero normal components enforced on the stress tensor, and distinguish between interior and boundary vertices. Let $k := p$ and set

$$\Sigma_h^a := \{\boldsymbol{\tau}_h \in \mathbf{S}_h^{\text{AFW}}(\omega_a) \mid \boldsymbol{\tau}_h \mathbf{n}_{\omega_a} = \mathbf{0} \text{ on } \partial\omega_a \quad \text{if } a \in \mathcal{V}_h^{\text{int}}, \quad (17a)$$

$$\boldsymbol{\tau}_h \mathbf{n}_{\omega_a} = \mathbf{0} \text{ on } \partial\omega_a \setminus \partial\Omega \quad \text{if } a \in \mathcal{V}_h^{\text{ext}}\},$$

$$\mathbf{V}_h^a := \{\mathbf{v}_h \in \mathbf{V}_h^{\text{AFW}}(\omega_a) \mid (\mathbf{v}_h, \mathbf{z})_{\omega_a} = 0 \quad \forall \mathbf{z} \in \mathbf{RM} \text{ if } a \in \mathcal{V}_h^{\text{int}}\}, \quad (17b)$$

$$\Lambda_h^a := \Lambda_h(\omega_a). \quad (17c)$$

Construction 2 (AFW stress reconstruction) Find $\boldsymbol{\sigma}_h^a \in \Sigma_h^a$, $\mathbf{r}_h^a \in \mathbf{V}_h^a$ and $\lambda_h^a \in \Lambda_h^a$ such that for all $(\boldsymbol{\tau}_h, \mathbf{v}_h, \boldsymbol{\mu}_h) \in \Sigma_h^a \times \mathbf{V}_h^a \times \Lambda_h^a$,

$$(\boldsymbol{\sigma}_h^a, \boldsymbol{\tau}_h)_{\omega_a} + (\mathbf{r}_h^a, \nabla \cdot \boldsymbol{\tau}_h)_{\omega_a} + (\lambda_h^a, \boldsymbol{\tau}_h)_{\omega_a} = (\boldsymbol{\psi}_a \boldsymbol{\sigma}(\mathbf{u}_h), \boldsymbol{\tau}_h)_{\omega_a}, \quad (18a)$$

$$(\nabla \cdot \boldsymbol{\sigma}_h^a, \mathbf{v}_h)_{\omega_a} = (-\boldsymbol{\psi}_a \mathbf{f} + \boldsymbol{\sigma}(\mathbf{u}_h) \nabla \boldsymbol{\psi}_a, \mathbf{v}_h)_{\omega_a}, \quad (18b)$$

$$(\boldsymbol{\sigma}_h^a, \boldsymbol{\mu}_h)_{\omega_a} = 0. \quad (18c)$$

Then, extending $\boldsymbol{\sigma}_h^a$ by zero outside ω_a , set $\boldsymbol{\sigma}_h := \sum_{a \in \mathcal{V}_h} \boldsymbol{\sigma}_h^a$.

Using the definitions (17), the formulation (18) is equivalent to a modified version of (9), adding the weak symmetry constraint (18c). The condition (15) for all $a \in \mathcal{V}_h^{\text{int}}$ ensures that the constrained minimization problem (18) is well-posed.

4.3 Properties of the Stress Reconstructions

For both stress reconstructions we obtain the following result, recalling that we assume \mathbf{f} to be piecewise polynomial of degree $p - 1$.

Lemma 1 (Properties of $\boldsymbol{\sigma}_h$). Let $\boldsymbol{\sigma}_h$ be prescribed by Construction 1 or Construction 2. Then $\boldsymbol{\sigma}_h \in \mathbf{H}(\text{div}, \Omega)$, and for all $T \in \mathcal{T}_h$, the following holds:

h^{-1}	estimate AFW		estimate AW		$\ \mathbf{u} - \mathbf{u}_h\ _{\text{en}}$		$I_{\text{eff,AFW}}$	$I_{\text{eff,AW}}$
4	1.707e-2	—	1.707e-2	—	1.704e-2	—	1.00	1.00
8	4.141e-3	2.05	4.124e-3	2.05	4.026e-3	2.08	1.03	1.02
16	1.175e-3	1.82	1.120e-3	1.88	1.116e-3	1.85	1.05	1.00
32	2.835e-4	2.05	2.736e-4	2.03	2.707e-4	2.04	1.05	1.01
64	7.384e-5	1.94	7.244e-5	1.92	7.021e-5	1.95	1.05	1.03

Table 1 Error estimators, analytical error, and effectivity indices under space refinement

$$\mathbf{f} + \nabla \cdot \boldsymbol{\sigma}_h = 0. \quad (19)$$

Proof. All the fields $\boldsymbol{\sigma}_h^a$ are in $\mathbf{H}(\text{div}, \omega_a)$ and satisfy appropriate zero normal conditions so that their zero-extension to Ω is in $\mathbf{H}(\text{div}, \Omega)$. Hence, $\boldsymbol{\sigma}_h \in \mathbf{H}(\text{div}, \Omega)$. Let us prove (19). Since (15) holds for all $a \in \mathcal{Y}_h^{\text{int}}$, we infer that (14b) or (18b) is actually true for all $\mathbf{v}_h \in \mathbf{V}_h(\omega_a)$. The same holds if $a \in \mathcal{Y}_h^{\text{ext}}$ by definition of \mathbf{V}_h^a . Hence, $(\boldsymbol{\psi}_a \mathbf{f} + \nabla \cdot \boldsymbol{\sigma}_h^a, \mathbf{v}_h)_{\omega_a} = 0$ for all $\mathbf{v}_h \in \mathbf{V}_h(\omega_a)$ and all $a \in \mathcal{Y}_h$. Since $\mathbf{V}_h(\omega_a)$ is composed of piecewise polynomials that can be chosen independently in each cell $T \in \mathcal{T}_a$, and using $\boldsymbol{\sigma}_h|_T = \sum_{a \in \mathcal{Y}_T} \boldsymbol{\sigma}_h^a|_T$ and the partition of unity $\sum_{a \in \mathcal{Y}_T} \boldsymbol{\psi}_a = 1$, we infer that $(\mathbf{f} + \nabla \cdot \boldsymbol{\sigma}_h, \mathbf{v}) = 0$ for all $\mathbf{v} \in \mathbf{V}_T$ and all $T \in \mathcal{T}_h$. The fact that $(\mathbf{f} + \nabla \cdot \boldsymbol{\sigma}_h)|_T \in \mathbf{V}_T$ for any $T \in \mathcal{T}_h$, concludes the proof. \square

5 Numerical Results

We illustrate numerically our theoretical results on a test case with a known analytical solution. We analyze the convergence rates of the error estimates and compare them to those of the analytical error. The computations were performed using the Code_Aster¹ software. The exact solution $\mathbf{u} = (u_x, u_y)$ on the unit square $\Omega = (0, 1)^2$ is given by

$$u_x = \frac{1}{\pi} \sin(\pi x) \cos(\pi y), \quad u_y = -\frac{1}{\pi} \sin(\pi x) \cos(\pi y),$$

with the Lamé parameters $\mu = \lambda = 1$, and the corresponding body force \mathbf{f} . The exact solution is imposed as Dirichlet condition on the whole boundary $\partial\Omega$. The discretization is done on a series of unstructured grids with the polynomial degree $p = 2$ in the conforming finite element method (3). For each computation, two error estimates are calculated, one for each stress reconstruction. The AFW reconstruction offers some advantages over the AW one: it is cheaper (since by hybridization techniques we can avoid the resolution of saddle point problems), and the implementation for three-dimensional problems is easier (the lowest-order AW element in 3D has 162 degrees of freedom per element).

¹ <http://web-code-aster.org>

Table 1 shows the error estimates calculated using the stress reconstruction in the AFW (Const. 2) and in the AW spaces (Const. 1), the analytical error in the energy norm, as well as their convergence rates. The two columns on the right indicate the effectivity indices (overestimation factors) for both reconstruction methods, calculated as the ratio of the estimate to the analytical error. Since we chose $p = 2$, the convergence rates are close to 2, with the rates of the estimates reproducing very closely the ones of the actual error. Furthermore, the effectivity indices close to 1 indicate the reliability of the estimates.

References

1. Ainsworth, M., Rankin, R.: Realistic computable error bounds for three dimensional finite element analyses in linear elasticity. *Comput. Methods Appl. Mech. Engrg.* **200**(21–22), 1909–1926 (2011)
2. Arnold, D.N., Falk, R.S., Winther, R.: Mixed finite element methods for linear elasticity with weakly imposed symmetry. *Math. Comput.* **76**, 1699–1723 (2007)
3. Arnold, D.N., Winther, R.: Mixed finite elements for elasticity. *Numer. Math.* **92**, 401–419 (2002)
4. Braess, D., Pillwein, V., Schöberl, J.: Equilibrated residual error estimates are p -robust. *Comput. Methods Appl. Mech. Engrg.* **198**, 1189–1197 (2009)
5. Braess, D., Schöberl, J.: Equilibrated residual error estimator for edge elements. *Math. Comp.* **77**(262), 651–672 (2008)
6. Brezzi, F., Douglas, J., Marini, L.D.: Recent results on mixed finite element methods for second order elliptic problems. In: D. Balakrishnan, L. Eds. (eds.) *Vistas in applied mathematics. Numerical analysis, atmospheric sciences, immunology*, pp. 25–43. Optimization Software Inc., Publications Division, New York (1986)
7. Cermak, M., Hecht, F., Tang, Z., Vohralík, M.: Adaptive inexact iterative algorithms based on polynomial-degree-robust a posteriori estimates for the Stokes problem (2017). HAL Preprint 01097662, submitted for publication
8. Destuynder, P., Métivet, B.: Explicit error bounds in a conforming finite element method. *Math. Comput.* **68**(228), 1379–1396 (1999)
9. Dörsek, P., Melenk, J.: Symmetry-free, p -robust equilibrated error indication for the hp -version of the FEM in nearly incompressible linear elasticity. *Comput. Methods Appl. Math.* **13**, 291–304 (2013)
10. Ern, A., Vohralík, M.: Adaptive inexact Newton methods with a posteriori stopping criteria for nonlinear diffusion PDEs. *SIAM J. Sci. Comput.* **35**(4), A1761–A1791 (2013)
11. Ern, A., Vohralík, M.: Polynomial-degree-robust a posteriori estimates in a unified setting for conforming, nonconforming, discontinuous Galerkin, and mixed discretizations. *SIAM J. Numer. Anal.* **53**(2), 1058–1081 (2015)
12. Kim, K.: A posteriori error estimator for linear elasticity based on nonsymmetric stress tensor approximation. *J. Korean Soc. Ind. Appl. Math.* **16**(1), 1–13 (2012)
13. Ladevèze, P., Leguillon, D.: Error estimate procedure in the finite element method and applications. *SIAM J. Numer. Anal.* **20**, 485–509 (1983)
14. Nicaise, S., Witowski, K., Wohlmuth, B.: An a posteriori error estimator for the Lamé equation based on $H(\text{div})$ -conforming stress approximations. *IMA J. Numer. Anal.* **28**, 331–353 (2008)
15. Riedlbeck, R., Di Pietro, D.A., Ern, A., Granet, S., Kazymyrenko, K.: Stress and flux reconstruction in Biot’s poro-elasticity problem with application to a posteriori analysis. to appear in *Comp. Math. Appl.* (2017). HAL Preprint 01366646